

The Eta Carinae 2009 Campaign

M. F. Corcoran^{1,2}

¹ CRESST/NASA-GSFC, Greenbelt MD USA

² Universities Space Research Association, Columbia, MD USA

Abstract: In January 2009, the enigmatic, extremely massive and luminous star η Car went through one of its periodic “minimum” states in which the excitation of its circumstellar nebula, along with the 2–10 keV emission from the star, collapses for a brief period. Current understanding associates this minimum state with the occurrence of periastron passage of a massive, unseen hot companion star around the much more luminous, much more massive η Car. These events offer a direct probe of the mass loss from η Car and the system as a whole, with circumstantial evidence tying these events to the spectacular “Great” and “Lesser” eruptions of the 19th century. As such these events have attracted the interest of a broad community of stellar and nebular astrophysicists. I report here on the results obtained during a nearly pan-chromatic campaign of observations of the January 2009 minimum, with some emphasis on the unique aspects of this particular minimum.

1 Introduction

Eta Car (η Car) is the closest example of a superluminous, supermassive star near $100M_{\odot}$ (Davidson & Humphreys 1997, Hillier et al. 2001). The star is near the Eddington limit and the Humphreys-Davidson limit, and as such it is very unstable. During the “Great Eruption” around 1843, η Car generated massive ejecta at speeds of up to 6000 km s^{-1} , producing almost as much kinetic energy as a low-luminosity supernova (Smith 2008) and producing the enormous bipolar circumstellar shell around the star, the so-called Homunculus Nebula. The star underwent a smaller, though still spectacular “Lesser” eruption in 1890. The physical cause of these eruptions is still not understood after 150 years of study. Nor is it understood what role such sporadic, large-scale eruptions play in driving the ultimate evolution of η Car, and those extremely massive objects like it, through hypernova and black hole formation.

Understanding these sporadic variations is difficult without identifying any type of underlying periodic phenomena. Astronomers have long sought periodicities in η Car’s observable behavior ever since the Great Eruption. Shortly after the Great Eruption, Rudolf Wolf and Elias Loomis suggested recurrence cycles of 46 and 67 years (Wolf 1863, Loomis 1869); more recently, shorter cycles of 15–16 years (Payne-Gaposchkin 1957) to 3 years (Feinstein & Marraco 1974) were also suggested. The complex behavior of η Car’s observed variations in broad-band photometry and in spectrographic observations made determination of any true period difficult, and none of these suggested periods had much predictive power.

The discovery of η Car’s first confirmed period depended on observations spanning twenty years or more. This began with the recognition of a so-called “spectroscopic event” by Zanella, Wolf and

Table 1: System parameters for the η Car binary system. Personal estimates for the types of observations providing the firmest estimates of these parameters are given: X=X-ray, U=ultraviolet, V=visible-band, I=IR.

Parameter	Value
P	2024 ± 2 days (X, U, V, I)
V_{∞} (η Car)	500 km s^{-1} (U,V)
V_{∞} (Companion)	3000 km s^{-1} (X)
$M_{\eta \text{ Car}}$	10^{-3} to 10^{-4} (U,V; X)
$M_{\text{companion}}$	10^{-5} (X)
e	0.9 (X,U,V)
a	15 AU? (X, U, V)
ω	$270^\circ?$, $90^\circ?$, $180^\circ?$... (X,U,V)
$\theta = 0$ (periastron passage)	$\phi = 0$ (start of X-ray minimum)
i	45° – $55^\circ?$ (U,V)

Stahl in 1981 (Zanella et al. 1984). These “events” represent a dramatic and complex change in η Car’s visible-band spectrum in which high-excitation He I and [Ne III] emission lines abruptly fade, then recover. Similar changes happened in 1948 and 1965, which suggested to them a recurrence timescale of 17 years (Zanella et al. 1984). We now recognize that other such events had occurred in 1953, 1959, 1970, and 1975. Near-infrared photometry from South Africa obtained by Patricia Whitelock and her collaborators (Whitelock et al. 1994) over 156 nights in 1975-1994 showed a significant 5–6 year cycle, but this cycle was confused with other near-infrared variations on other timescales. Meanwhile new spectroscopic events occurred in 1986 and in 1992, though the former was not widely reported.

The breakthrough was provided by a set of 27 measurements of the He I 10830Å emission line obtained by Augusto Damineli at Brazil’s National Astrophysical Laboratory. These observations, augmented by 4 additional measures from other observers from 1981–1995, showed a clear, rapid weakening of the 10830Å line every 5.5 years, lasting only for a few weeks (a duty cycle of < 5%). Damineli (1996) also showed the fading of the 10830Å line occurred at nearly the same time as brightening of the system in the near IR, and that the 5.5 year period recovered not only the “spectroscopic event” seen by Zanella, Wolf and Stahl in 1981, but also all other “spectroscopic events” observed in the previous 50 years, and perhaps even the Great Eruption in the 1840’s and the Lesser Eruption of 1890. Serendipitous observations of η Car during 1992–1993 at the Australian Telescope National Facility (Duncan et al. 1995) and by the Röntgen Satellite (Corcoran et al. 1995) confirmed the presence of a minimum state in the radio and X-ray bands. Damineli’s period (which has now been refined to $P = 2024 \pm 2$ days, Damineli et al. 2008) successfully predicted the occurrence of the next minimum at the end of 1997, an event which was observed in the radio to optical through the UV up to the X-ray regime.

Orbital motion of one star around another provides the simplest interpretation of this strict, panchromatic period. The long period and short duty cycle of the minimum suggests that the orbit is highly eccentric ($e \sim 0.8$ – 0.9), and further suggests that the minima occur near periastron passage when the stars are moving most rapidly. The response of the circumstellar Homunculus nebula around the cycle suggests variable photo-excitation and photo-ionization conditions in the nebula. This is now attributed to photospheric radiation from a companion star much hotter than η Car, whose radiation gets funneled by a “bow shock” produced by the collision of the companion’s wind with the stronger wind of η Car. The minimum state occurs as the companion’s emission is blocked by the inner wind of

η Car near periastron passage. A simulation of the expected density distribution of the two interacting winds at certain key times in the orbit is shown in Figure 1.

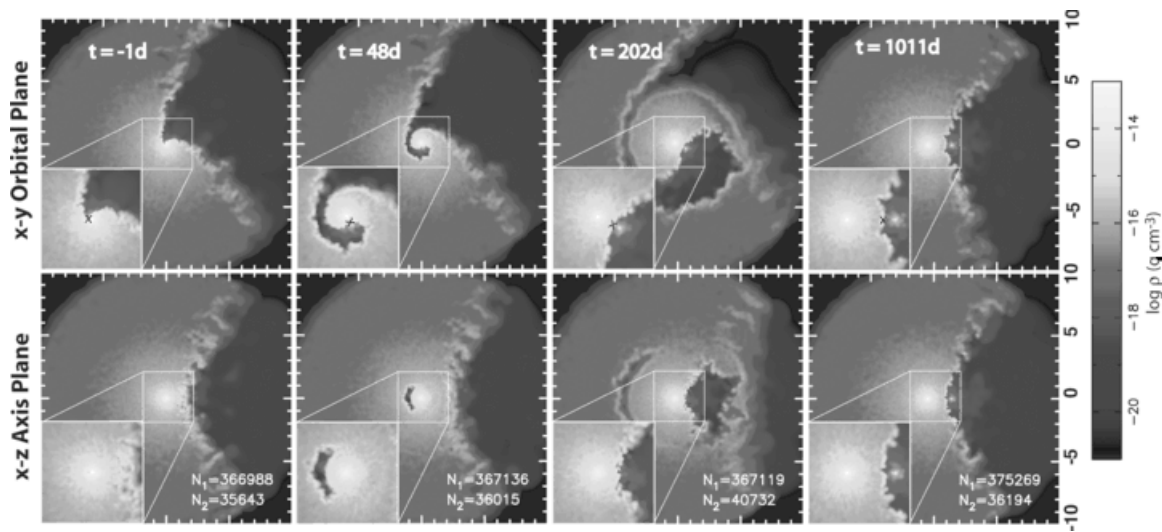


Figure 1: “Snapshots” of the wind density distribution in and perpendicular to the orbital plan from a 3-D smoothed particle hydrodynamics (SPH) simulation by Okazaki et al. (2008) for selected times in the 2024-day orbit. The “bow shock” is concave around the weaker-wind companion star. X-ray emission originates along the bow shock on the side of the companion star, and most of the far UV photospheric radiation from the companion star can only escape through the lower-density companion wind bounded by the bow shock.

We note that there is as yet no widely accepted direct evidence of the companion star (however, see for example, Iping et al. 2005). Arguably, the best evidence of the presence of a companion star in orbit around η Car comes from study of the 2–10 keV X-ray emission variations. Detailed X-ray observations (Ishibashi et al. 1999, Corcoran 2005) document a variation that is most easily explained as originating in shock-heated gas produced where a fast ($V \approx 3000 \text{ km s}^{-1}$), less dense wind of a companion star slams into the slow ($V \approx 500 \text{ km s}^{-1}$), dense wind from η Car. The parameters of the system are given in Table 1, along with a personal estimate of the wavebands used to derive these parameters. The first three parameters are rather firmly established, while there is some uncertainty in the remainder.

2 The 2009 Minimum

Damineli’s ephemeris predicted a minimum on January 16, 2009 (oddly enough, just days after a similar event in WR140, another long-period highly eccentric massive binary, which is the topic of a review by Williams 2011). In anticipation of this event, observations spanning almost the entire electromagnetic spectrum were planned. Although a number of observers frequently monitor η Car whenever feasible, we consider the observing campaign as beginning roughly one year before the predicted minimum (January 2008), when most of the new observations began in earnest. Although much progress had been made from prior observations, especially during the 2003 July minimum (which included detailed observations with the Hubble Space Telescope obtained as part of the HST η Car Treasury Program¹) there were a number of key issues left unresolved. What actually causes the “event” (an eclipse?; cooling/“discombobulation” of the shock?; phase-dependent mass loss?; jet

¹<http://etacar.umn.edu/>

formation?), and is the wind-wind collision region stable? Do the stars interact near periastron, and if so how? How is the geometry of the inner wind of η Car altered by the passage of the companion through it, and how does this geometry propagate outwards? What is the actual density profile of η Car's wind? And most importantly, what are the stellar radial velocities and what is the system mass ratio? Addressing these questions was a main goal of the 2009 η Car observing campaign, with the hope of reconstructing the full 3-D geometry of the wind-driven mass loss from the system.

3 The Campaigners

Table 2 gives a list of participants in the 2009 observing campaign. This list is incomplete, because it's impossible to identify everyone who made significant contributions in the space allotted, but hopefully, it captures much of the observational effort. It's divided by energy band and since it's observationally biased, it ignores the significant modelling efforts of Pittard, Parkin, Okazaki, Madura, Russell, Soker, Kashi and Akashi. Some of the modeling work is described elsewhere in this volume.

Table 2: An (incomplete) list of Participants in the η Car 2009 Observing Campaign

Regime	Observatory	Observers
Hard X-ray/ Gamma Ray (> 10 keV - 300 GeV)	INTEGRAL, Fermi, AGILE, Suzaku	Leyder et al., Takahashi/Fermi Team, Tavani et al., Hamaguchi et al., Russell et al.
X-ray (1-10 keV)	RXTE, Chandra, Suzaku, XMM, Swift	Corcoran, Hamaguchi et al., Pian et al.
UV/Optical	OPD-LNA/Brazil, SOAR, HST, OALP, CASLEO, SMARTS/CTIO, Monash, VLT/UVES, Magellan	Damineli, Mairan et al., Mehner, Davidson et al., Gull, Madura et al., Fernandez-Lajus et al., Gies, Richardson et al., Landes & Fitzgerald, Bomans, Weis, Stahl
IR	VLT/AMBER, VLT/CRIRES, VLT/VINCI	Weigelt et al., Groh et al.
(sub)mm	Itapetinga, APEX	Abraham et al., Gomez et al.
Radio	ATNF	White

4 Results

In the following section we highlight some of the main observational results.

4.1 Broad-Band Monitoring in the Optical and X-ray Bands

Figure 2 compares photometry of the system in two wavebands: ground-based V-band photometry from the LaPlata group (Fernández-Lajús et al. 2010) and space-based 2–10 keV X-ray photometry from the *RXTE* satellite (Corcoran et al. 2010). Both the optical and X-ray monitoring have similar sampling and similar spectral sensitivity. Nominally, the optical data has much better spatial resolving power compared to the X-ray data (12'' vs. 1° for the *RXTE* Proportional Counter Array), but the X-ray

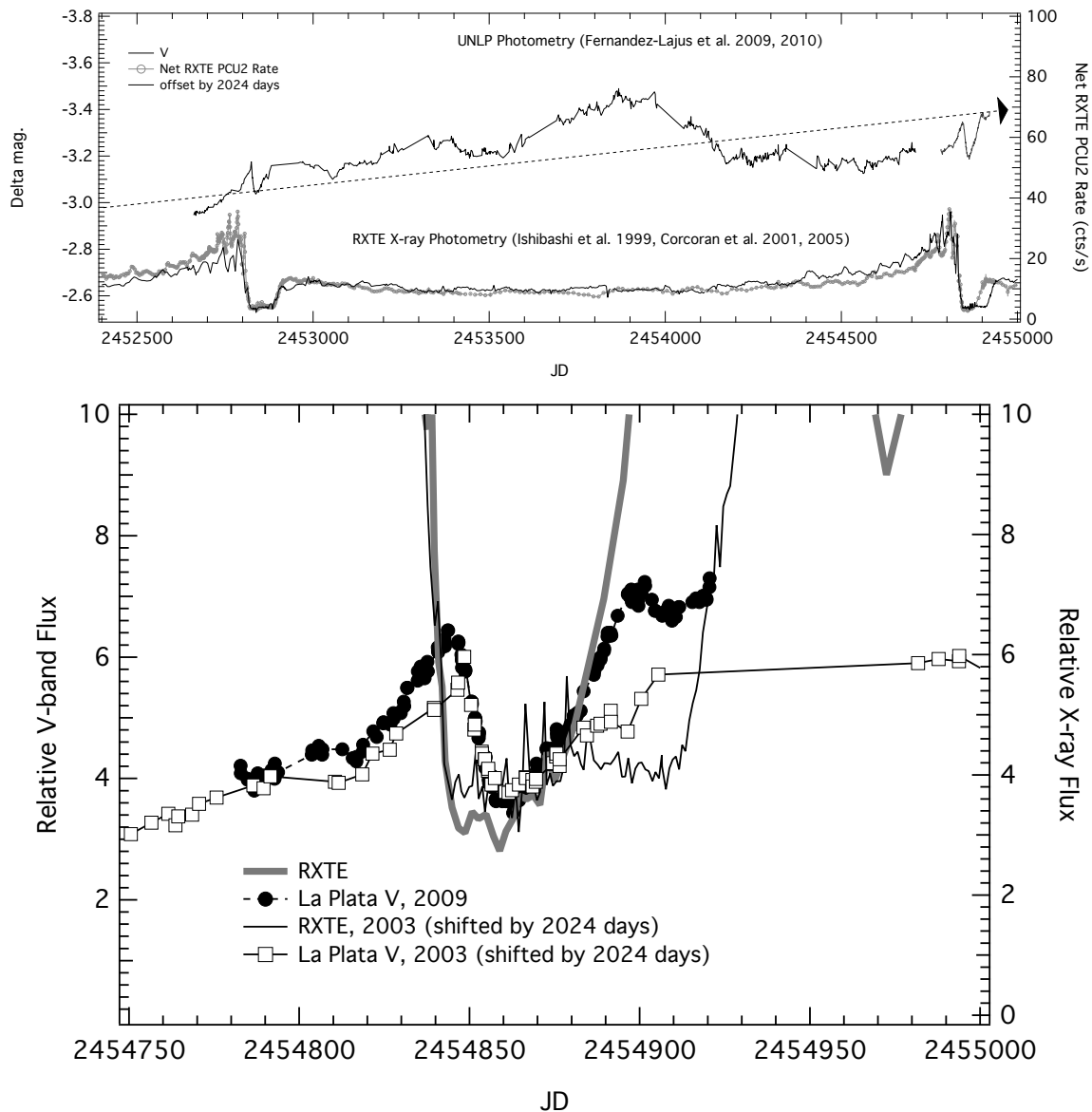


Figure 2: Top: Comparison of V-band photometry by the La Plata group from the Virpi S. Niemela telescope at LaPlata and at CASLEO covering the 2003.5 and 2009 minima, compared to the 2–10 keV band X-ray photometry from *RXTE*. The dashed arrow represents the general brightening trend at V seen in recent years. Both the V-band and 2–10 keV emission show evidence of “eclipse-like” minima, though the relative depth is much more pronounced in the X-ray band. Bottom: A detailed comparison of the V-band and X-ray flux variations for both minima. The 2003.5 data for both the X-ray and V photometry has been progressed forward by 2024 days for comparison with the 2009 minimum.

emission arises in a limited volume in the bow shock where the winds collide and so should sample a much smaller region of variability than the optical photometry does. As can be seen in the figure, an “eclipse-like” minimum is apparent from both ground and space, though the relative variation is larger in the X-ray data than in the optical. The optical emission is confused between real intrinsic changes in stellar brightness and circumstellar changes in the environment of the Homunculus. This confusion accounts for some of the large-scale variations seen in the V-band lightcurve. A particularly interesting feature is the large “hump” between JD 2453500 and 2454200. No such change is seen

in the X-ray lightcurve during this interval. The bottom panel of Figure 2 shows a detailed view of the two minima sampled by the X-ray and optical monitoring. Both show good reproducibility in the decline to the minimum, particularly impressive in light of the relative lack of correlation between the X-ray and V band outside of the minimum. The comparison of the 2003 and 2009 X-ray minima show that the 2009 minimum was substantially shorter than the 2003 minimum by about 1 month. There is also some evidence that the optical “eclipse” was also shorter in 2009 than in 2003, as indicated in Figure 2. The question is, what caused the minima (so stable in 1998 and 2003) to be so much shorter in 2009?

4.2 A Sea Change?

Since the minimum is strongly influenced by the density of η Car’s wind, it’s perhaps reasonable to suggest that shorter minimum duration means that the density of the wind has changed (Kashi & Soker 2009, Corcoran et al. 2010). One way to determine the overall mass loss rate from η Car is to examine the strengths of H α and other strong emission lines. Mehner et al. (2010) compared a set of strong emission lines from η Car (particularly Fe II, [Fe II], Cr II, [Cr II] and H α) obtained at approximately the same phase in the 5.5-year cycle but separated by 2 cycles. They found that, compared to 1999, the continuum-normalized emission lines decreased by factors of order 2 in 2010, (for example, see the H α profiles in Figure 3). The simplest explanation of this large scale decrease in emission line strength is a recent, significant decrease in the density of the wind from η Car. Preliminary modeling of the X-ray data suggests that a large change in wind density (equivalent to a factor of 2 or more decline in η Car’s mass-loss rate) is necessary to explain the narrow 2009 X-ray minimum. It’s unclear if the decline in emission line strength documented by Mehner et al. is consistent with so large a change in wind density. Nevertheless these data do suggest some type of large intrinsic change in η Car is occurring.

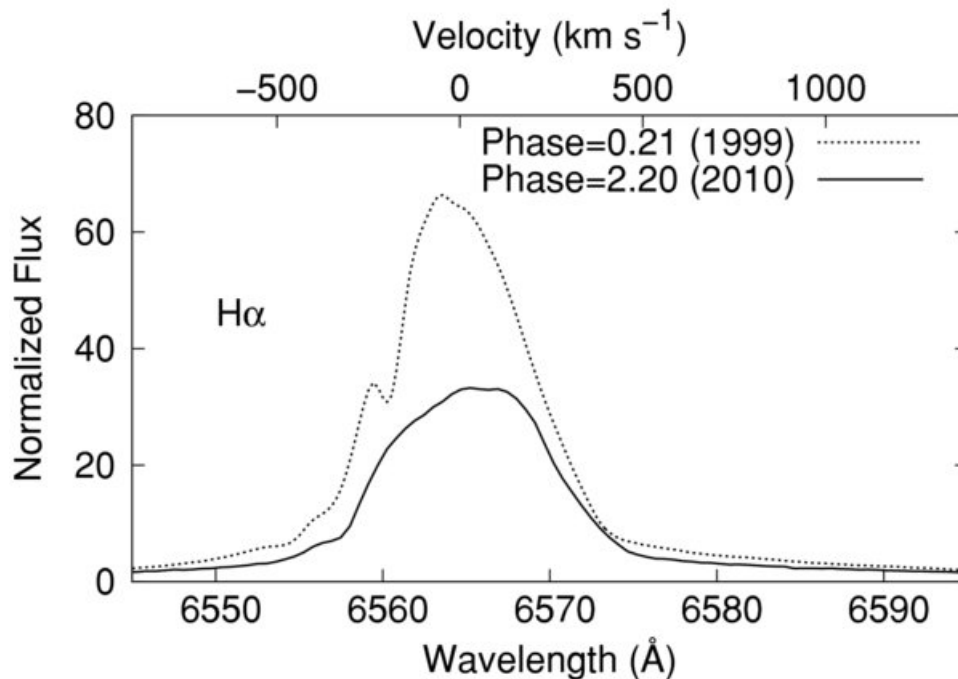


Figure 3: Comparison of the H α line profile from η Car 1999 & 2010 (Mehner et al. 2010).

4.3 High-Velocity Outflows

The appearance of high velocity emission in the X-ray emission line spectrum was noted by Behar et al. (2007) and Henley et al. (2008) using *CHANDRA* grating observations obtained just prior to the X-ray minimum in 2003. X-ray line profiles showed emission at velocities $V \approx -2000 \text{ km s}^{-1}$. Such velocities are about a factor of 2–4 \times higher than the wind speed of η Car, but somewhat lower than the deduced companion wind speed (speeds of $\approx 3000 \text{ km s}^{-1}$ are necessary to produce the observed X-ray emission at energies above 3 keV, Pittard & Corcoran 2002). The 2003 observations left unclear whether this high velocity emission represented a transient jet from the poles of the companion or the projected outflow from the wind-shock region. The upper panel of Figure 4 compares the Ly α profiles from the strong hydrogenic Si XIV line obtained between 20–40 days before the X-ray minima in 2003 and 2009, along with the same line at apastron. In contrast to the apastron profile, the profiles of the Si XIV emission near both the 2000 and 2009 minima are broader and show blue-shifted emission to velocities of $\approx -2000 \text{ km s}^{-1}$. However, the centroid velocity peak in 2009 is at a substantially lower velocity compared to the 2003 profile.

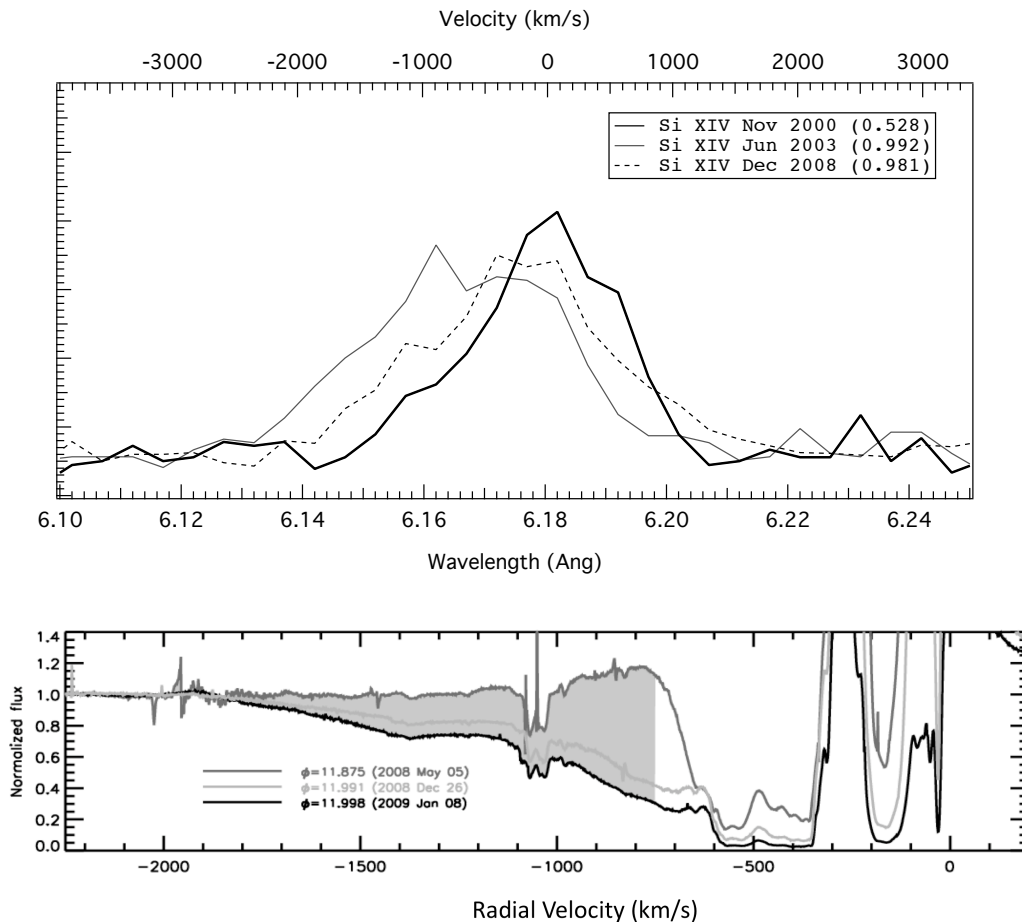


Figure 4: Top: comparison of Ly α Si XIV line profiles from *CHANDRA* High Energy Transmission Grating spectra just prior to X-ray minimum in 2003 (thin solid line) and 2008 (dashed line); the thick line shows the Si XIV Ly α line near apastron from 2000 November for reference. Bottom: variation of the He I 10830 Å line from CRIRES spectra (Groh et al. 2010) in 2008-2009.

Similar changes can be seen at lower energies. Groh et al. (2010) obtained a detailed series of measures of the He I 10830 Å line from 2008 through 2009 with the Cryogenic high-resolution InfraRed Echelle Spectrograph (CRIRES). These observations clearly showed the appearance, in absorption,

of high velocity material appearing about 1 month prior to the 2009 X-ray minimum, i.e. consistent with the appearance of the high-velocity X-ray emission. The lower panel of Figure 4 shows the development of the high velocity absorption component in 2008 December and 2009 January from Groh et al. (2010). They also noted the appearance in HST/STIS data from 2003 of high velocity absorption in the Si IV resonance doublet at 1400\AA in a similar interval prior to the 2003 minimum. They further showed that no such high-velocity emission was seen in lower ionization species. This is strong evidence that the high-velocity features seen in the X-ray, near-IR and UV regions trace the outflow along the wind-wind shock, and thus can be used to constrain models of velocity and ionization changes with distance along the wind-wind bow shock. Such information is crucial to understanding the geometry of the bow shock and the relative strength of the stellar winds from the two stars.

4.4 The Shape of Things – To Come?

As the bow shock swings around following the companion star in its orbit, the companion's far UV photospheric radiation variably illuminates the circumstellar gas and dust like a cosmic searchlight. This variable illumination in principle constrains the shape of the bow shock, the orbital motion and also the geometric distribution of the outer wind and ejecta around η Car. This can provide information about the mass-loss rates of both stars, help constrain the mass ratio, and refine our understanding of the sporadic large-scale ejection events. Therefore this is a dynamic area of current research. Figure 5 shows a simulation of a spatially-resolved [Fe III] emission line at 4659\AA based on the distorted outer wind of η Car from a 3-D SPH simulation (Madura, 2010, PhD thesis; see also the discussion by Madura et al. 2011). This simulation is then compared to the same line profile as observed by HST/STIS (Gull et al. 2009).

Madura found that the simulation which best matched the observed STIS profile had $i \approx 40^\circ \pm 10^\circ$, $\omega \approx 255^\circ \pm 15^\circ$, with the orbital axis projected on the sky at a position angle $\Theta \approx 312^\circ \pm 15^\circ$. This implies that the orbital angular momentum vector is closely aligned with the symmetry axis of the Homunculus, with the resulting projected orbit on the sky having the companion star moving clockwise around η Car, with apastron on the observer's side of the system. This orientation is shown on the bottom panel of Figure 5.

The size of the emitting region has been imaged interferometrically at 2 microns by Weigelt and collaborators using the Very Large Telescope Interferometer. During the 2009 minimum, the size of the He I emitting region collapsed from 17.4 mas (39 AU) to only 5.7 mas (13AU) on 5 Jan 2009 (see Figure 6) before recovering in 2009 March to 11 mas (25 AU). Even at minimum, the size of the emitting region is apparently still comparable to the size of the orbital semi-major axis (~ 16 AU). Throughout this interval, the size of the Br- γ and continuum-emitting region stayed almost constant. On 2009 March 3 the size of the He I emitting region recovered to 11.4 mas (25 AU).

4.5 Even Higher Energy Emission

Studies of η Car at hard X-ray and Gamma-ray energies have been made using *INTEGRAL*, *AGILE*, *Suzaku*, and *Fermi*. At these energies emission is dominated by non-thermal processes like inverse Compton scattering or synchrotron emission. *INTEGRAL*, *AGILE*, and *Fermi* all have directly imaged a strong source within a few arcminutes of η Car (see Figure 7). The source is rather luminous with $L_\gamma \approx 10^{34}$ ergs s^{-1} in the 20-100 keV band, increasing to $\approx 10^{36}$ ergs s^{-1} in the 1-300 GeV band. There is as yet no strong suggestion that the Gamma-ray source varies through the minimum, though the statistical significance of the observations are not exceedingly high. Tavani et al. (2009) reported the occurrence of a Gamma-ray flare by *AGILE* which was not however confirmed by contempora-

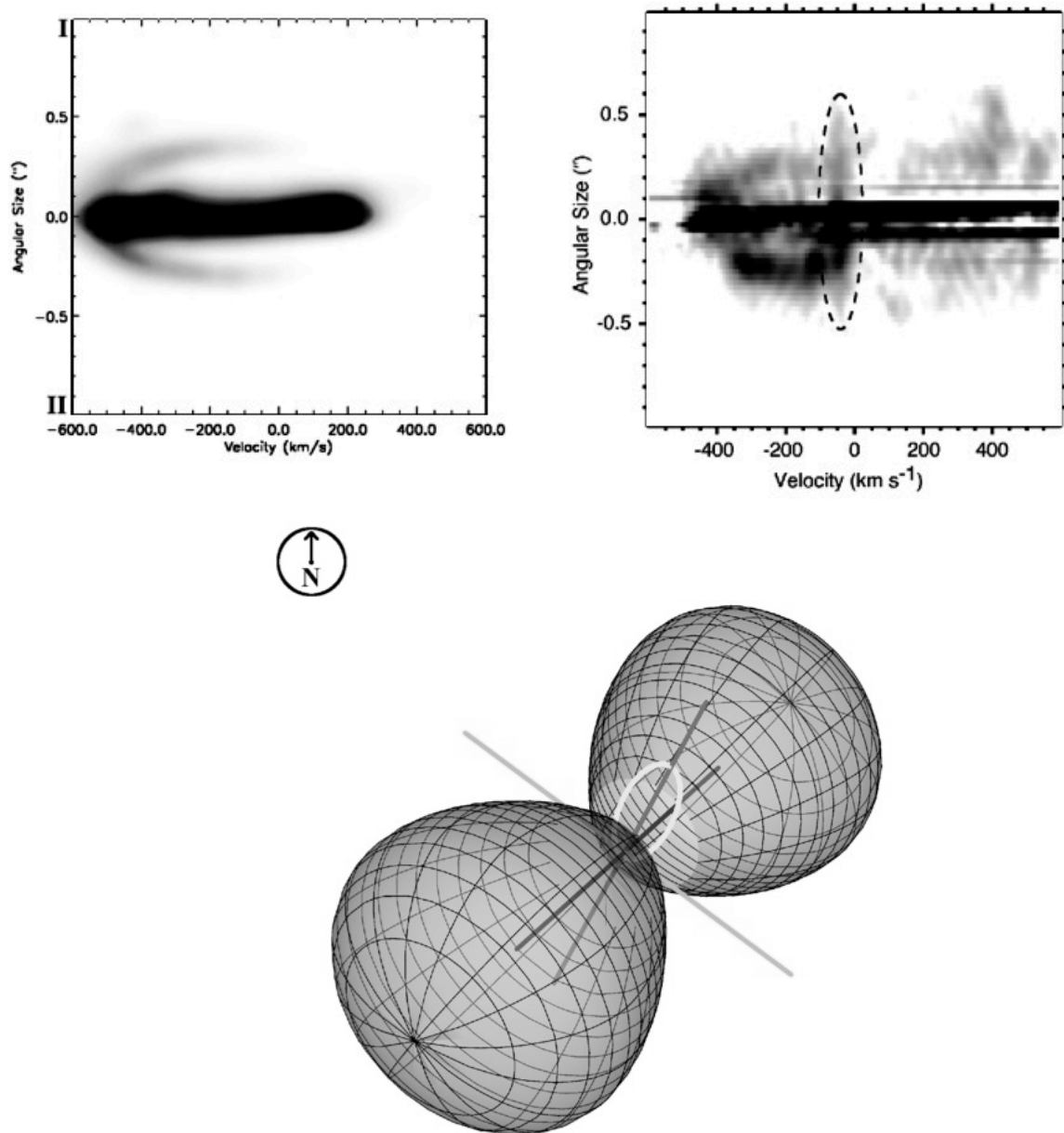


Figure 5: Top left: simulated spatially resolved [Fe III] line profile by Madura et al. (2011) for a particular slit orientation based on a 3-D SPH model. Top right: Observed spatially-resolved line profile as observed by HST/STIS for the same slit orientation (Gull et al. 2009). The simulation successfully reproduces the overall shape and orientation of the [Fe III] emission line as observed by STIS for the particular slit position and orbital phase of the observation. The dotted oval shows the region of emission produced by one of the “Weigelt knots” (a dense nebulosity ejected from the star in the 19th century) and is not included in the model simulation. Bottom: a “dressmaker’s dummy” model of the orbital orientation based on the line profile simulation showing the relation of the derived orbit relative to the orientation of the bipolar lobes of the Homunculus (not to scale).

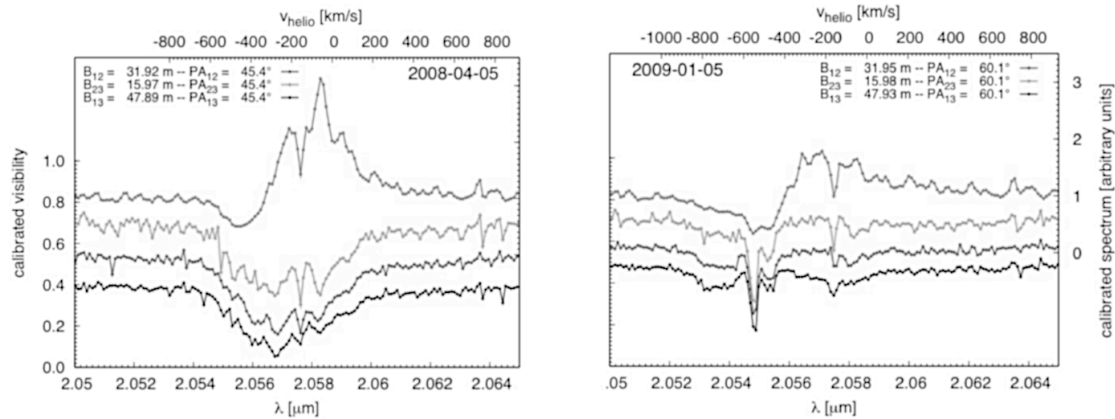


Figure 6: Visibilities at He I $2.06\mu\text{m}$ obtained at the VLTI from 2008 (*left*) and in 2009 January (*right*). The He I emitting region collapsed from 17.4 mas (39 AU) to 5 mas (11 AU) in 2009 January, and grew to 11 mas by 2009 March.

neous observations with *Fermi*. It is possible that the observed Gamma-ray source is not directly associated with the stellar source; perhaps it's associated somehow with the ejecta (see, for example, Ohm et al. 2010), or perhaps arises from an unrelated background object (though the almost perfect coincidence with η Car seems to rule out a chance alignment with a background source).

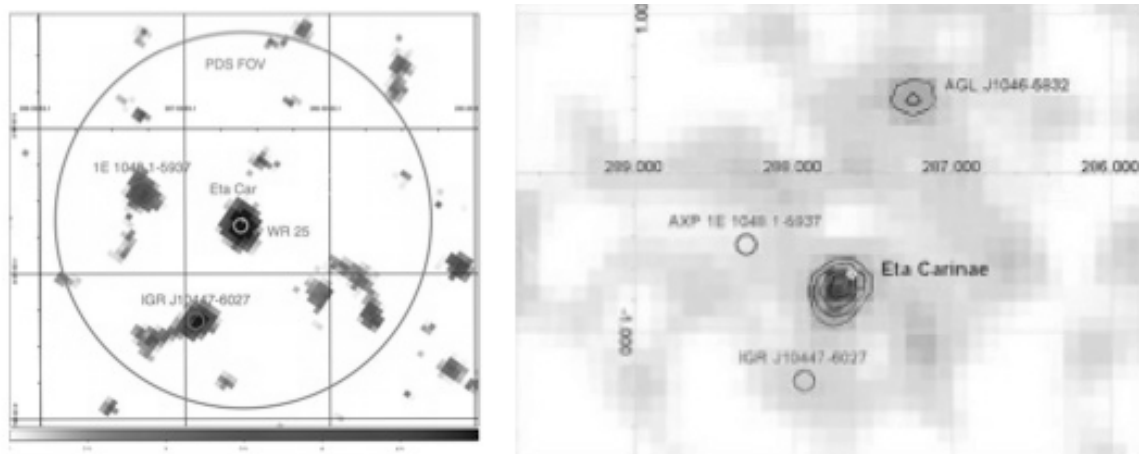


Figure 7: Left: an *INTEGRAL*-ISGRI image of the field around η Car, in the 20-100 keV band (Leyder et al. 2008). A significant source is detected near η Car. Right: an *AGILE* observation of η Car in the 30 MeV–30 GeV band (Tavani et al. 2009).

5 Conclusions and Possible Directions for Future Work

Arguably the most surprising result of the 2009 observing campaign was the rapid recovery from the minimum state seen most prominently at X-ray energies, along with the decline in emission line strength seen in the optical. The cause of these changes is still not well understood, although a decline in the mass loss rate from η Car itself likely plays a significant role. But if so then preliminary modeling of the X-ray minimum duration suggests a large change in mass loss rate (by a factor of 2–4 or so) is required. It remains to be seen if such a large change is consistent with the decline in emission line strength reported by Mehner et al. (2010); if not this either means that the emitting

material producing the optical emission lines and the 2–10 keV X-rays may originate in different volumes with different densities, or something even stranger is going on. But if the mass loss rate really declined by a factor of 2 or more, then this must be driven by some fundamental, underlying change in the photospheric radiation field of the star itself. What this could be remains to be examined.

Attempts to image the system, either interferometrically or by examining the response of the distorted wind to illumination by the far UV of the companion via spatially-resolved spectrometry and 3-D modeling, hold great hope to advance our understanding of the physical parameters of the stars and to refine the orbital elements. This work already supports a fundamental correlation between the orbit of the system and the ejection of the material that formed the Homunculus, helping to strengthen ties between periastron passage and the mechanism producing (or at least shaping) the Great Eruption.

Clearly, new observations are needed to understand the future evolution of mass loss from the system and to understand fully the mass-loss history. Modeling efforts, especially in 3-D, including realistic heating and cooling mechanisms, and including adaptive methods to try to resolve the structure of the bow shock, also provide an important key for interpreting the anticipated wealth of new data (and to better understand the legacy data residing in the η Car Treasury Program archives and in the high energy archives). One wonders what changes 2014 will bring.

Acknowledgements

I'd like to acknowledge the immense efforts of this world-wide group in carrying out this observing campaign and the extraordinary efforts undertaken in order to increase our understanding of this peculiar and spectacular object. In particular I need to gratefully thank those observers and modelers who have graciously shared their results, in many cases prior to publication. I'd also like to acknowledge the contributions of all those who were not specifically noted in this report due to space limitations. The *CHANDRA* η Car program has been supported by *CHANDRA* grants GO0-11039A, G07-8022A, G09-0016A, and G08-9018A. This support is gratefully acknowledged. This work has also been supported in part by NASA Cooperative Agreement NNG06EO90A. This research has made use of NASA's Astrophysics Data System Bibliographic Services, an indispensable tool. This research has made use of data obtained from the High Energy Astrophysics Science Archive Research Center (HEASARC), provided by NASA's Goddard Space Flight Center, also an indispensable resource for the high energy astrophysicist.

References

- Behar, E., Nordon, R., & Soker, N. 2007, *ApJL*, 666, L97
Corcoran, M. F. 2005, *AJ*, 129, 2018
Corcoran, M. F., Rawley, G. L., Swank, J. H., & Petre, R. 1995, *ApJL*, 445, L121
Corcoran, M.F., Hamaguchi, K., Pittard, J.M., Russell, C.M.P., Owocki, S.P., Parkin, E.R., & Okazaki, A. 2010, *ApJ*, 725, 1528
Damineli, A. 1996, *ApJL*, 460, L49
Damineli, A., Hillier, D. J., Corcoran, M. F., et al. 2008, *MNRAS*, 386, 2330
Davidson, K., & Humphreys, R. M. 1997, *ARAA*, 35, 1
Duncan, R. A., White, S. M., Lim, J., Nelson, G. J., Drake, S. A., & Kundu, M. R. 1995, *ApJL*, 441, L73
Feinstein, A., & Marraco, H. G. 1974, *A&A*, 30, 271
Fernández-Lajús, E., Fariña, C., Calderón, J. P., et al. 2010, *New Astronomy*, 15, 108
Groh, J. H., Nielsen, K. E., Damineli, A., et al. 2010, *A&A*, 517, A9+
Gull, T. R., Nielsen, K. E., Corcoran, M. F., et al. 2009, *MNRAS*, 396, 1308
Henley, D. B., Corcoran, M. F., Pittard, J. M., Stevens, I. R., Hamaguchi, K., & Gull, T. R. 2008, *ApJ*, 680, 705
Hillier, D. J., Davidson, K., Ishibashi, K., & Gull, T. 2001, *ApJ*, 553, 837

- Iping, R. C., Sonneborn, G., Gull, T. R., Massa, D. L., & Hillier, D. J. 2005, ApJL, 633, L37
Ishibashi, K., Corcoran, M. F., Davidson, K., et al. 1999, ApJ, 524, 983
Kashi, A., & Soker, N. 2009, ApJL, 701, L59
Leyder, J.-C., Walter, R., & Rauw, G. 2008, A&A, 477, L29
Loomis, E. 1869, MNRAS, 29, 298
Madura, T.I., Gull, T.R., Owocki, S.P., Okazaki, A.T., & Russell, C.M.P. 2011, in Proceedings of the 39th Liège Astrophysical Colloquium, eds. G. Rauw, M. De Becker, Y. Nazé, J.-M. Vreux & P.M. Williams, BSRSL 80, 694
Mehner, A., Davidson, K., Humphreys, R. M., et al. 2010, ApJL, 717, L22
Ohm, S., Hinton, J. A., & Domainko, W. 2010, ApJL, 718, L161
Okazaki, A. T., Owocki, S. P., Russell, C. M. P., & Corcoran, M. F. 2008, MNRAS, 388, L39
Payne-Gaposchkin, C. 1957, The Galactic Novae (Amsterdam: North-Holland Pub. Co.)
Pittard, J. M., & Corcoran, M. F. 2002, A&A, 383, 636
Smith, N. 2008, Nature, 455, 201
Tavani, M., Sabatini, S., Pian, E., et al. 2009, ApJL, 698, L142
Whitelock, P. A., Feast, M. W., Koen, C., Roberts, G., & Carter, B. S. 1994, MNRAS, 270, 364
Williams, P.M. 2011, in Proceedings of the 39th Liège Astrophysical Colloquium, eds. G. Rauw, M. De Becker, Y. Nazé, J.-M. Vreux & P.M. Williams, BSRSL 80, 595
Wolf, R. 1863, Astronomische Nachrichten, 60, 59
Zanella, R., Wolf, B., & Stahl, O. 1984, A&A, 137, 79

Discussion

N. Smith: From the near-IR SED, we see that the new dust forming in the wind collision is very hot - about 1700 K. That means it can't be silicates (which form at ≤ 1000 K) like the dust in the Homunculus. The hot dust could be carbon-rich, except that we think Eta Car's wind is N-rich and C/O-poor. Thus, the newly forming dust is probably corundum (Al_2O_3) or something similar, which can condense at high temperatures.

D. Gies: Would the general brightening taking place at the current epoch be inconsistent with a decrease in the LBV mass loss rate?

M. Corcoran: Not necessarily. The extinction is decreasing mostly caused by the expansion of the Homunculus.